On Full Multigrid Schemes for Isogeometric Analysis

Clemens Hofreither[1] and Walter Zulehner[1]

Abstract We investigate a geometric full multigrid method for solving the large sparse linear systems which arise in isogeometric discretizations of elliptic partial differential equations. We observe that the full multigrid approach performs much better than the V-cycle multigrid method in many cases, in particular in higher dimensions with increased spline degrees. Often, a single cycle of the full multigrid process is sufficient to obtain a quasi-optimal solution in the L_2-norm. A modest increase in the number of smoothing steps suffices to restore optimality in cases where the V-cycle performs badly.

1 Introduction

Isogeometric analysis (IGA), a numerical technique for the solution of partial differential equations first proposed in Hughes et al. [2005], has attracted considerable research attention in recent years. The use of spline spaces both for representation of the geometry and for approximation of the solution affords the method several very interesting features, such as the possibility to use exactly the geometry generated by CAD systems, refinement without further communication with the CAD system, the possibility of using high-continuity trial functions, the use of high-degree spaces with comparatively few degrees of freedom, and more. We refer to Hughes et al. [2005], Bazilevs et al. [2006] as well as the monograph Cottrell et al. [2009] and the references therein for details on this method.

The efficient solution of the discretized systems arising in isogeometric analysis has been the topic of several publications, among these, Collier et al. [2012], Kleiss et al. [2012], da Veiga et al. [2012], Gahalaut et al. [2013],

Institute of Computational Mathematics, Johannes Kepler University Linz, Altenbergerstr. 69, 4040 Linz, Austria chofreither@numa.uni-linz.ac.at · zulehner@numa.uni-linz.ac.at

da Veiga et al. [2013], Buffa et al. [2013]. In the present paper, we investigate geometric full multigrid methods for IGA. It is known (Gahalaut et al. [2013]) that geometric multigrid solvers for IGA possess h-independent convergence rates for V-cycle iteration using standard smoothers. Our aim is to study more closely the performance of the full multigrid (FMG) iteration strategy, especially in dependence of the spline degree.

2 Isogeometric analysis

We construct, in every direction $i = 1, \dots, d$, a B-spline space of degree p_i over an open knot vector which spans the parameter interval $(0, 1)$. *Open* means that the first and last knots are repeated $p_i + 1$ times. We restrict ourselves to maximum continuity, i.e., all knots in the interior are simple. For the definition of B-splines, see, e.g., Schumaker [2007], Piegl and Tiller [1997], Cottrell et al. [2009]. Taking the tensor product of the B-splines bases over all directions i, we obtain a tensor product basis $\{B_j : (0,1)^d \to \mathbb{R}_0^+\}_j$. To each of its basis functions B_j, we associate a control point (coefficient) $C_j \in \mathbb{R}^d$ in such a way that we obtain an invertible geometry mapping $F = \sum_j C_j B_j : (0,1)^d \to \Omega$, where $\Omega \subset \mathbb{R}^d$ is the computational domain. The isogeometric basis functions on Ω are given by $B_j \circ F^{-1} : \Omega \to \mathbb{R}_0^+$, and their span is the isogeometric trial space on Ω.

In practice, NURBS, i.e., rational versions of the B-spline basis functions, are commonly used to represent the geometry. In this paper, we however restrict ourselves to the case of B-splines for the sake of simplicity.

In the following, let $\mathcal{V}_h \subset H_0^1(\Omega)$ denote a tensor product spline space over Ω as constructed above. An isogeometric method for the Poisson equation with Dirichlet boundary conditions is given by the discrete variational problem: find $u_h \in \mathcal{V}_h$ such that, for all $v_h \in \mathcal{V}_h$,

$$\int_\Omega \nabla u \cdot \nabla v \, dx =: a(u_h, v_h) = \langle F, v_h \rangle := \int_\Omega f v_h \, dx - a(\tilde{g}, v),$$

where $\tilde{g} \in H^1(\Omega)$ is a suitable extension of the Dirichlet data g. Here, $u_h + \tilde{g}$ is the approximation to the solution of the boundary value problem.

Essential boundary conditions require some care in isogeometric methods. In our setting, we construct an approximation g_h to g which lies in the spline space. Due to the use of open knot vectors, the degrees of freedom (DoFs) can be cleanly separated into boundary DoFs and interior DoFs. The values for the boundary DoFs of g_h are determined by solving a $(d-1)$-dimensional Lagrange interpolation problem on each face of the patch Ω, where the Gréville points of the spline basis are chosen as interpolation points. The interior DoFs of g_h are set to zero. In the variational setting, this corresponds to solving a problem with the approximate right-hand side

$$\langle F_h, v\rangle = \int_\Omega f v \, dx - a(g_h, v). \tag{1}$$

On the topic of essential boundary conditions in isogeometric analysis, we also refer to Wang and Xuan [2010], Mitchell et al. [2011], Chen et al. [2011].

3 Geometric multigrid methods for IGA

In the following, we outline very briefly the construction of a geometric multigrid scheme for IGA. We refer to the multigrid literature (Hackbusch [2003], Briggs et al. [2000], Trottenberg et al. [2000]) for further details.

Starting from a coarse isogeometric mesh, inserting a new knot at the midpoint of every non-empty knot span creates a "fine" spline space with a halved mesh size which contains all functions of the original "coarse" spline space, yielding the isogeometric analogue of uniform h-refinement.

Let $\hat{\mathcal{V}}_0$ denote a coarse parametric spline space over $(0,1)^d$ which is rich enough to represent the geometry Ω exactly. With repeated uniform refinement steps, we obtain a sequence of h-refined spline spaces $\hat{\mathcal{V}}_1, \hat{\mathcal{V}}_2, \ldots$ The push-forward to the geometry yields isogeometric spline spaces $\mathcal{V}_0, \mathcal{V}_1, \mathcal{V}_2, \ldots$

Let $\mathcal{V}_H \subset \mathcal{V}_h$ denote two successive spline spaces with the canonical embedding $P : \mathcal{V}_H \to \mathcal{V}_h$. One step of the two-grid iteration process is given by a pre-smoothing step, the coarse-grid correction, and a post-smoothing step. Given a starting value $u_0 \in \mathcal{V}_h$, the next iterate u_1 is thus obtained from

$$\begin{aligned} u^{(1)} &:= u_0 + M^{-1}(f_h - A_h u_0), \\ u^{(2)} &:= u^{(1)} + P A_H^{-1} P^\top (f_h - A_h u^{(1)}), \\ u_1 := u^{(3)} &:= u^{(2)} + M^{-\top}(f_h - A_h u^{(2)}). \end{aligned}$$

Here, M is a suitable smoother for the fine-space stiffness matrix A_h. Common choices are the Richardson smoother (with M being a scalar multiple of identity), the damped Jacobi smoother (M being a scaled diagonal of A_h), and the Gauss-Seidel smoother (M being the lower triangular part of A_h). A multigrid scheme is obtained by considering a hierarchy of nested spline spaces and replacing the exact inverse A_H^{-1} in the above procedure recursively with the same procedure applied on the next coarser space, until $\mathcal{V}_0$ is reached, where an exact solver is used.

We set up a Poisson model problem, $-\Delta u = f$, with pure Dirichlet boundary conditions on the d-dimensional unit interval $\Omega = (0,1)^d$. We choose tensor product B-spline basis functions defined on equidistant knot vectors with constant spline degrees $p_1 = \ldots = p_d = p$ and maximum continuity. The geometry mapping F is chosen as identity. The right-hand side f and the boundary conditions are chosen according to the prescribed analytical solution $u(x) = \prod_{i=1}^d \sin(\pi(x_i + 0.5))$.

As a comparison point, we test the V-cycle iteration numbers. For this, we choose a random starting vector u_0 and perform V-cycle iteration until the initial residual is reduced by a factor of 10^{-8} in the Euclidean norm. The resulting iteration numbers are shown in Table 1. We point out that very similar numbers have been obtained in Gahalaut et al. [2013]. In higher dimensions, in particular for $d = 3$, the number of iterations sees a dramatic increase as the spline degree is raised.

d	N	p				d	N	p				d	N	p			
		1	2	3	4			1	2	3	4			1	2	3	4
	∼500	11	9	7	10		∼4k	9	12	37	140		∼6k	9	37	249	1935
1	∼4.1k	11	8	7	9	2	∼66k	9	11	37	127	3	∼40k	9	38	240	1682
	∼262k	11	8	7	9		∼1.05m	9	11	36	125		∼290k	9	38	236	1564

Table 1 V-cycle iteration numbers for the model Poisson problem. Columns, left to right: space dimension d, number of unknowns N, V-cycle iteration numbers for $p = 1$ to 4.

4 Full multigrid for IGA

We set up a full multigrid (FMG) method in the usual way. That is, we start from the exact coarse-grid solution $u_0 = A_0^{-1} f_0 \in \mathcal{V}_0$ and transfer it to the next higher level by means of a full interpolation operator, $u_1 = I_0^1(u_0)$. Here the solution is corrected by one multigrid V-cycle with a suitable coarse-space right-hand side f_i, and the result is again interpolated to the next higher level by means of I_1^2. This procedure is continued until the finest space $\mathcal{V}_\ell$ is reached, where one final V-cycle is applied. We found that two issues related to the treatment of Dirichlet boundary conditions need attention.

First, we need a sequence of full interpolation operators $I_i^{i+1} : \mathcal{V}_i \to \mathcal{V}_{i+1}$ which transfer solutions, as opposed to mere corrections, to the next finer level while maintaining a high order of accuracy. Dirichlet boundary conditions must be carefully taken into account here. Recall that the approximation to the solution of the boundary value problem on level i is given by $u_i + g_i$, where g_i is a spline function approximating the Dirichlet boundary data having non-zero coefficients only on the boundary DoFs, whereas u_i vanishes on the boundary DoFs since they were eliminated from the linear system. Prolonging both contributions separately, we see that $P_i^{i+1} u_i \in \mathcal{V}_{i+1}$ still vanishes on the boundary DoFs. On the other hand, the representation of g_i in $\mathcal{V}_{i+1}$ has non-zero contributions in some interior DoFs close to the boundary. This situation is illustrated in the 1D setting in Figure 1. Therefore, the proper choice for the full interpolation operator is $I_i^{i+1}(u_i) := P_i^{i+1} u_i + \mathring{P}_i^{i+1} g_i$, where by $\mathring{P}_i^{i+1}$ we mean the operator which prolongs the boundary function and discards the boundary DoFs, keeping only the contributions to the interior DoFs.

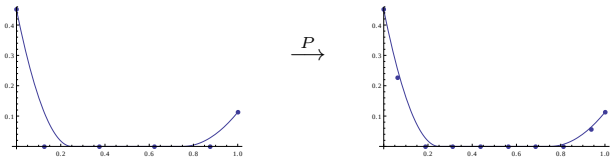

Fig. 1 Prolongation of boundary functions creates non-zero contributions to interior DoFs

The second issue is related to the choice of the coarse-space right-hand sides f_i, $i = 1, \ldots, \ell - 1$. The seemingly natural choice $f_i = (P_i^{i+1})^\top f_{i+1}$ does not take into account that the right-hand side vector f_ℓ stems from the approximated linear functional $\langle F_h, \cdot \rangle$ given in (1), where we have chosen a fine-grid spline approximation g_h for the Dirichlet data. This approximation by necessity depends on the mesh level: the fine-grid Dirichlet functions must have better approximation properties, but cannot be represented on coarser grids. We thus found it necessary to assemble f_i on every level separately.

With these issues taken care of, we apply a single FMG cycle to the Poisson model problem introduced in Section 3 for different values of the space dimension d, the spline degree p and the problem size N and compute the resulting L_2-error with respect to the exact solution. The errors are presented in Tables 2–4 for the 1D, 2D and 3D cases along with the error ratio between successive refinement levels. (In some cases, the errors stagnate once a threshold sufficiently close to the machine accuracy is reached due to rounding errors.) From the approximation properties derived in Bazilevs et al. [2006], we would hope for an error which asymptotically behaves like $\mathcal{O}(h^{p+1})$. We observe that this behavior is achieved using a single FMG cycle for all tested spline degrees up to 4 in the 1D case, and for degrees up to 3 in the 2D and 3D cases. One possible measure to restore the optimal convergence orders in the case $p = 4$ is to increase the number of pre- and postsmoothing steps. In Table 5, we display the resulting errors with 2 smoothing steps in 2D and with 3 smoothing steps in 3D.

We remark that the solution time using the FMG method was typically only a small fraction of the time used to assemble the problems.

Acknowledgments

This work was supported by the National Research Network "Geometry + Simulation" (NFN S117, 2012–2016), funded by the Austrian Science Fund (FWF). The first author was also supported by the project AComIn "Advanced Computing for Innovation", grant 316087, funded by the FP7 Capacity Programme "Research Potential of Convergence Regions".

$p=1$			$p=2$		
N	L_2-error	ratio	N	L_2-error	ratio
33	$4.944858 \cdot 10^{-4}$	4.76	34	$3.722578 \cdot 10^{-6}$	8.09
65	$1.034253 \cdot 10^{-4}$	4.78	66	$4.646054 \cdot 10^{-7}$	8.01
129	$2.231043 \cdot 10^{-5}$	4.64	130	$5.808685 \cdot 10^{-8}$	8.00
257	$5.090763 \cdot 10^{-6}$	4.38	258	$7.263190 \cdot 10^{-9}$	8.00
513	$1.218115 \cdot 10^{-6}$	4.18	514	$9.081029 \cdot 10^{-10}$	8.00
$p=3$			$p=4$		
N	L_2-error	ratio	N	L_2-error	ratio
35	$6.536758 \cdot 10^{-8}$	16.71	36	$4.984064 \cdot 10^{-9}$	34.42
67	$3.966554 \cdot 10^{-9}$	16.48	68	$1.527129 \cdot 10^{-10}$	32.64
131	$2.439422 \cdot 10^{-10}$	16.26	132	$4.754326 \cdot 10^{-12}$	32.12
259	$1.512164 \cdot 10^{-11}$	16.13	260	$1.750396 \cdot 10^{-13}$	27.16
515	$9.883776 \cdot 10^{-13}$	15.30	516	$9.712425 \cdot 10^{-14}$	1.80

Table 2 Errors after one full multigrid cycle in 1D.

$p=1$			$p=2$		
N	L_2-error	ratio	N	L_2-error	ratio
4225	$1.76004 \cdot 10^{-4}$	4.20	4356	$4.8427 \cdot 10^{-7}$	8.05
16641	$4.28888 \cdot 10^{-5}$	4.10	16900	$6.0407 \cdot 10^{-8}$	8.02
66049	$1.05903 \cdot 10^{-5}$	4.05	66564	$7.5446 \cdot 10^{-9}$	8.01
263169	$2.63839 \cdot 10^{-6}$	4.01	264196	$9.4271 \cdot 10^{-10}$	8.00
1050625	$6.59801 \cdot 10^{-7}$	4.00	1052676	$1.1782 \cdot 10^{-10}$	8.00
$p=3$			$p=4$		
N	L_2-error	ratio	N	L_2-error	ratio
4489	$6.8025 \cdot 10^{-9}$	17.47	4624	$1.2380 \cdot 10^{-9}$	28.05
17161	$3.8527 \cdot 10^{-10}$	17.66	17424	$6.1208 \cdot 10^{-11}$	20.23
67081	$2.2387 \cdot 10^{-11}$	17.21	67600	$3.6698 \cdot 10^{-12}$	16.68
265225	$1.3527 \cdot 10^{-12}$	16.55	266256	$2.4967 \cdot 10^{-13}$	14.70
1054729	$2.6654 \cdot 10^{-13}$	5.07			

Table 3 Errors after one full multigrid cycle in 2D.

$p=1$			$p=2$		
N	L_2-error	ratio	N	L_2-error	ratio
125	$7.2738 \cdot 10^{-2}$	—	216	$3.0617 \cdot 10^{-3}$	—
729	$1.2829 \cdot 10^{-2}$	5.67	1000	$2.0613 \cdot 10^{-4}$	14.85
4913	$3.2797 \cdot 10^{-3}$	3.91	5832	$2.4836 \cdot 10^{-5}$	8.30
35937	$7.9084 \cdot 10^{-4}$	4.15	39304	$3.5042 \cdot 10^{-6}$	7.09
274625	$1.9521 \cdot 10^{-4}$	4.05	287496	$4.3712 \cdot 10^{-7}$	8.02
$p=3$			$p=4$		
N	L_2-error	ratio	N	L_2-error	ratio
343	$4.5383 \cdot 10^{-4}$	—	512	$1.1096 \cdot 10^{-4}$	—
1331	$5.4518 \cdot 10^{-5}$	8.32	1728	$2.5938 \cdot 10^{-5}$	4.28
6859	$3.4414 \cdot 10^{-6}$	15.84	8000	$3.1818 \cdot 10^{-6}$	8.15
42875	$1.8704 \cdot 10^{-7}$	18.40	46656	$1.9189 \cdot 10^{-7}$	16.58
300763	$1.0657 \cdot 10^{-8}$	17.55	314432	$9.5155 \cdot 10^{-9}$	20.17

Table 4 Errors after one full multigrid cycle in 3D.

$d=2,\nu=2$	N	L_2-error	ratio
	64	$7.809885 \cdot 10^{-5}$	—
	144	$4.964622 \cdot 10^{-6}$	15.75
	400	$1.426569 \cdot 10^{-7}$	34.80
	1296	$3.616898 \cdot 10^{-9}$	39.44
	4624	$8.554892 \cdot 10^{-11}$	42.28
	17424	$2.027914 \cdot 10^{-12}$	42.19
	67600	$5.222339 \cdot 10^{-14}$	38.83
	266256	$1.010133 \cdot 10^{-13}$	0.52
$d=3,\nu=3$	N	L_2-error	ratio
	512	$6.282724 \cdot 10^{-5}$	—
	1728	$3.377428 \cdot 10^{-6}$	18.60
	8000	$1.116225 \cdot 10^{-7}$	30.26
	46656	$2.372285 \cdot 10^{-9}$	47.05

Table 5 Errors for $p = 4$ after one FMG cycle with ν pre- and postsmoothing steps.

References

Y. Bazilevs, L. Beirão da Veiga, J. A. Cottrell, T. J. R. Hughes, and G. Sangalli. Isogeometric analysis: approximation, stability and error estimates for h-refined meshes. *Mathematical Models and Methods in Applied Sciences*, 16(07):1031–1090, 2006.

W. L. Briggs, V. E. Henson, and S. F. McCormick. *A Multigrid Tutorial*. Society for Industrial and Applied Mathematics, 2000. ISBN 9780898714623.

A. Buffa, H. Harbrecht, A. Kunoth, and G. Sangalli. BPX-preconditioning for isogeometric analysis. *Computer Methods in Applied Mechanics and Engineering*, 265:63–70, 2013. ISSN 0045-7825. doi: 10.1016/j.cma.2013.05.014.

T. Chen, R. Mo, and Z. W. Gong. Imposing Essential Boundary Conditions in Isogeometric Analysis with Nitsche's Method. *Applied Mechanics and Materials*, 121–126:2779–2783, October 2011. doi: 10.4028/www.scientific.net/AMM.121-126.2779.

N. Collier, D. Pardo, L. Dalcin, M. Paszynski, and V. M. Calo. The cost of continuity: A study of the performance of isogeometric finite elements using direct solvers. *Computer Methods in Applied Mechanics and Engineering*, 213–216:353–361, 2012. ISSN 0045-7825. doi: 10.1016/j.cma.2011.11.002. URL `http://www.sciencedirect.com/science/article/pii/S0045782511003392`.

J. A. Cottrell, T. J. R. Hughes, and Y. Bazilevs. *Isogeometric Analysis: Toward Integration of CAD and FEA*. John Wiley & Sons, Chichester, England, 2009.

L. Beirão da Veiga, D. Cho, L. Pavarino, and S. Scacchi. Overlapping Schwarz methods for isogeometric analysis. *SIAM Journal on Numerical Analysis*, 50(3):1394–1416, 2012. doi: 10.1137/110833476. URL `http://epubs.siam.org/doi/abs/10.1137/110833476`.

L. Beirão da Veiga, D. Cho, L. Pavarino, and S. Scacchi. BDDC preconditioners for isogeometric analysis. *Mathematical Models and Methods in Applied Sciences*, 23(6):1099–1142, 2013. doi: 10.1142/S0218202513500048.

K. P. S. Gahalaut, J. K. Kraus, and S. K. Tomar. Multigrid methods for isogeometric discretization. *Computer Methods in Applied Mechanics and Engineering*, 253:413–425, 2013. ISSN 0045-7825. doi: 10.1016/j.cma.2012.08.015. URL http://www.sciencedirect.com/science/article/pii/S0045782512002678.

W. Hackbusch. *Multi-Grid Methods and Applications*, volume 4 of *Springer Series in Computational Mathematics*. Springer-Verlag, Berlin, Heidelberg, New York, Tokyo, 2003.

T. J. R. Hughes, J. A. Cottrell, and Y. Bazilevs. Isogeometric analysis: CAD, finite elements, NURBS, exact geometry and mesh refinement. *Computer Methods in Applied Mechanics and Engineering*, 194(39-41):4135–4195, October 2005. ISSN 00457825. doi: 10.1016/j.cma.2004.10.008. URL http://dx.doi.org/10.1016/j.cma.2004.10.008.

S. K. Kleiss, C. Pechstein, B. Jüttler, and S. Tomar. IETI – Isogeometric tearing and interconnecting. *Computer Methods in Applied Mechanics and Engineering*, 247–248:201–215, 2012. ISSN 0045-7825. doi: 10.1016/j.cma.2012.08.007.

T. J. Mitchell, S. Govindjee, and R. L. Taylor. A method for enforcement of Dirichlet boundary conditions in isogeometric analysis. In Dana Mueller-Hoeppe, Stefan Loehnert, and Stefanie Reese, editors, *Recent Developments and Innovative Applications in Computational Mechanics*, pages 283–293. Springer Berlin Heidelberg, 2011. ISBN 978-3-642-17483-4. doi: 10.1007/978-3-642-17484-1_32. URL http://dx.doi.org/10.1007/978-3-642-17484-1_32.

L. Piegl and W. Tiller. *The NURBS Book*. Monographs in visual communications. Springer-Verlag GmbH, 1997. ISBN 9783540615453.

L. Schumaker. *Spline Functions: Basic Theory*. Cambridge Mathematical Library. Cambridge University Press, 2007. ISBN 9780521705127.

U. Trottenberg, C.W. Oosterlee, and A. Schuller. *Multigrid*. Elsevier Science, 2000. ISBN 9780080479569.

D. Wang and J. Xuan. An improved NURBS-based isogeometric analysis with enhanced treatment of essential boundary conditions. *Computer Methods in Applied Mechanics and Engineering*, 199(37–40):2425–2436, 2010. ISSN 0045-7825. doi: http://dx.doi.org/10.1016/j.cma.2010.03.032. URL http://www.sciencedirect.com/science/article/pii/S004578251000109X.